

Nonperturbative $SU(3)$ thermodynamics and the phase transition

N.O. Agasian^{a,b,*}, M.S. Lukashov^{a,c,†} and Yu.A. Simonov^{a,‡}

^a *Alikhanov Institute for Theoretical and Experimental Physics,
Moscow 117218, Russia*

^b *National Research Nuclear University “MEPhI”,
Moscow 115409, Russia*

^c *Moscow Institute of Physics and Technology,
Dolgoprudny 141700, Moscow Region, Russia*

March 10, 2022

Abstract

The $SU(3)$ equation of state ($P(T)$, $s(T)$, $I(T)$) are calculated within the Field Correlator Method both in the confined and the deconfined phases. The basic dynamics in our approach is contained in the vacuum correlators, both of the color-electric (CE) and colormagnetic (CM) types, which ensure CE and CM confinement below T_c and CM confinement and Polyakov loops above T_c . The resulting values of T_c and $P(T)$, $I(T)$, $s(T)$ are in good agreement with lattice measurements.

*agasian@itep.ru

†lukashov@phystech.edu

‡simonov@itep.ru

1 Introduction

The dynamics of QCD at small temperatures is known to be governed by confinement, which establishes its scale, connected to the string tension σ , and this scale defines the nucleon mass and the most energy density of the visible part of the Universe.

The theory of confinement based on the vacuum averages of field correlators in QCD, was suggested in [1], see [2] for reviews.

The idea that QCD might have a different phase without confinement at large temperature, was suggested long ago [3, 4].

This deconfinement phase was studied in the same framework of the vacuum correlators, soon after the theory of confinement in [5], and it was finally elaborated in [6–8], see the review in [9], where numerical calculations were done and compared to existing data. The theory of temperature transition in QCD given in [6, 7] is easily generalized to the case of nonzero density [8].

The main idea of the temperature transition in QCD given in all these papers is based on two points:

1) From the basic thermodynamics law one can deduce, that the states with the minimal free energy (maximal pressure) are more probable. Therefore with the growing temperature the physical systems prefer configurations with reduced correlators and larger entropy. As the consequence the phase with zero colorelectric confining vacuum correlators and condensates (and nonzero colormagnetic) wins at some temperature, leading to the deconfining vacuum.

2) The lowest (also the dominant) Gaussian field correlators provide two basic interactions: the linear confining $V_D^{\text{lin}}(r) \sim \sigma r$ and two interactions with saturating maxima: $V_1(r, T)$ and $V_D^{\text{sat}}(r, T)$ where $V(\infty, T) \text{ const.}$ The latter yields automatically the Polyakov lines $L_a(T) = \exp\left(-\frac{c_a V_1(\infty, T)}{2T}\right)$, $c_3 = 1$, $c_8 = \frac{9}{4}$, which enter linearly the thermodynamic potential and suppress its magnitude. This is a basic point, since in our approach $L_a(T)$ appear necessarily in $F(T)$ as factors in the deconfinement phase, and it is not a model assumption.

As it was shown in [7], $L_a(T)$ alone give a reasonable (within 20-25%) description of the $P(T)$, $I(T)$ etc. in the deconfined phase, when all other nonperturbative (e.g. colormagnetic) contributions are neglected.

In addition, this lowest approximation used in [7], with free gluon and quark loops augmented by known Polyakov loops was able to predict the main rough characteristics, transition (crossover) temperature T_c and even its chemical potential dependence $T_c(\mu)$ [8], as well as pressure $P(T)$, trace anomaly $I(T) = \varepsilon - 3P$, sound velocity $c_s(T)$ [7] etc. with reasonable accuracy.

An interesting development of the same deconfinement theory is contained in [10, 11], where the influence of strong magnetic fields was taken into account, again in good agreement with lattice data.

It is a purpose of the present paper to make a step further, and to take into account another important nonperturbative (np) interaction: the colormagnetic confinement with the string tension σ_s . It was shown in [12] that it resolves the Linde problem [13, 14] and creates bound states in 3d [15]. Here we would like to study how it affects the pure SU(3) thermodynamic potentials, in particular $P(T)$, $I(T)$, latent heat, critical temperature T_c .

One of advantages of our analytic approach is that we can analyze the N_c behavior of all quantities and compare it to numerical studies [16, 17].

The SU(3) gluodynamics is an important testing ground for the theory, since it contains most np and perturbative characteristics of the full QCD. On the lattice side already the first studies [18–20] revealed the phase transition and important new physical effects both below and above T_c . On the perturbative side the resummation method of the Hard Thermal Loop (HTL), first developed in [21,22], was used in [23,24] in the SU(3) theory, demonstrating a good agreement with lattice data at large T , whereas at $T < 4T_c$ one needs np contributions. On the lattice side the most accurate data are obtained in [25], see also [26] for a recent publication. In an alternative way the $SU(3)$ thermodynamics was studied in the framework of effective theories in [27–34], in particular in the PNJL model in [32–34], while in [31] the author exploited the AdS/QCD formalism.

In what follows we shall start from the theory developed in [5–7], but make more explicit the dynamics in the confined and deconfined phases.

Note, that the basic ground for this deconfinement theory is already contained in the np confinement mechanism, suggested in [1].

In this approach the confinement is a result of the np color field correlators, which are vacuum averages of the Euclidean colorelectric (CE) and colormagnetic (CM) field $\langle \text{tr} E_i(x) E_j(y) \rangle$, $\langle \text{tr} H_i(x) H_j(y) \rangle$, proportional to functions (correlators) $D^E(x-y)$, $D_1^E(x-y)$ and $D^H(x-y)$, $D_1^H(x-y)$ respectively.

$$\begin{aligned} \frac{g^2}{N_c} \langle \langle \text{Tr} E_i(x) \Phi E_j(y) \Phi^\dagger \rangle \rangle &= \delta_{ij} \left(D^E(u) + D_1^E(u) + u_4^2 \frac{\partial D_1^E}{\partial u^2} \right) + u_i u_j \frac{\partial D_1^E}{\partial u^2}, \\ \frac{g^2}{N_c} \langle \langle \text{Tr} H_i(x) \Phi H_j(y) \Phi^\dagger \rangle \rangle &= \delta_{ij} \left(D^H(u) + D_1^H(u) + \mathbf{u}^2 \frac{\partial D_1^H}{\partial \mathbf{u}^2} \right) - u_i u_j \frac{\partial D_1^H}{\partial u^2}, \end{aligned} \quad (1)$$

Here $u = x - y$ and $\Phi(x, y) = P \exp(ig \int_y^x A_\mu dz_\mu)$ is the parallel transporter, needed to maintain the gauge invariance of relations (1).

The confining correlators D^E, D^H generate the nonzero values of CE and CM string tensions,

$$\sigma^{E(H)} = \frac{1}{2} \int D^{E(H)}(z) d^2 z. \quad (2)$$

At zero temperature T both string tensions coincide and σ^E forms the basic np scale, which defines all hadron masses and the QCD scale in general.

To make the theory selfconsistent, one must calculate $D^{E(H)}, D_1^{E(H)}$, via $\sigma^E = \sigma^H \equiv \sigma$ and prove that Eq.(2) is satisfied. This was done in [35], where it was shown that the correlators are proportional to the Green's functions of gluelumps, calculated before on the lattice [36] and analytically in the framework of our method [37].

The correlators D^E and D_1^E produce both the scalar confining interaction $V_D(r)$ and the vector-like interaction $V_1(r)$.

$$V_D(r) = 2c_a \int_0^r (r - \lambda) d\lambda \int_0^\infty d\nu D^E(\lambda, \nu) = V_D^{(\text{lin})}(r) + V_D^{(\text{sat})}(r) \quad (3)$$

$$V_1(r) = c_a \int_0^r \lambda d\lambda \int_0^\infty d\nu D_1^E(\lambda, \nu), \quad c_{\text{fund}} = 1, \quad c_{\text{adj}} = 9/4. \quad (4)$$

Separating from $V_D(r)$ the purely linear form $V_D^{(\text{lin})}(r)$ and using the renormalization procedure for $V_1(r)$ with account of the perturbative gluon exchange, $V_1(r) = V_1^{\text{sat}}(r) + V_{OGE}(r)$, one obtains the general structure of the $q\bar{q}$ or gg interaction in the region $T < T_c$.

$$V(r, T < T_c) = V_D^{\text{lin}}(r) + V_D^{\text{sat}}(r) + V_1^{\text{sat}}(r) + V_{\text{OGE}}(r). \quad (5)$$

It is interesting, that both parts, $V_D^{\text{sat}} + V_1^{\text{sat}}$, saturating at large r , compensate each other at small T , as shown in appendix, and one is retained with the standard linear + OGE interaction, in exact agreement with lattice and experiment.

However at $T \geq T_c$, when D^E vanishes, one obtains two terms, V_1^{sat} and V_{OGE} , which together with σ_s define the dynamics.

The np thermodynamics [7, 9] based on the field correlators (FC), considers the low temperature phase of SU(3), and of QCD in general, as the confined phase, where thermal degrees of freedom are white hadrons, glueballs in the SU(3) case, where all FC (D^E, D_1^E, D^H, D_1^H) are nonzero and therefore both CE and CM (spatial) confinement are present.

Since D_1^E is nonzero above T_c , one may associate with it and with D^H, D_1^H the deconfined phase (phase II), while the confined phase (phase I) contains all four correlators D^E, D_1^E, D^H, D_1^H , so that the phase transition can be found from the intersection of two curves $P_I(T)$ and $P_{II}(T)$, as shown in Fig.1 and will be demonstrated below.

In phase I the special role is played by $D^E(\sigma^E)$, which ensure not only confinement in the usual sense, but also chiral symmetry breaking (CSB), [38]. As mentioned above, the nonzero np part of D_1^E is almost totally compensated by D^E for $T < T_c$, while the perturbative part yields gluon exchange contribution. The CM correlators D^H, D_1^H ensure most part of spin-dependent forces [39] and CM confinement.

With the growth of T for $T < T_c$ nothing special happens, except that more and more excited states (glueballs in SU(3)) participate in the partition function, ensuring a steady but slow increase of the pressure $P_{\text{conf}} \equiv P_I(T)$ with T . This corresponds to the vacuum with all correlators nonzero.

An interesting feature of the glueball pressure P_{conf} is that the standard Hardron Resonance Gas (HRG) approach is not able to sustain the growth of P_{conf} near T_c and one is using the Hagedorn enhancement in addition to HRG to comply with the lattice data. We show in the paper, that instead of the Hagedorn factors, which we consider inappropriate to us, as will be discussed below, one can use the effect of string tension damping with temperature near T_c , observed on the lattice [40–42], which strongly increases P_{conf} at $T \lesssim T_c$ and brings it in agreement with lattice data [25].

The deconfined phase (phase II) corresponds to the zero values of D^E and σ^E , and nonzero D_1^E, D^H, D_1^H . In this case the physical degrees of freedom are gluons, interacting via these correlators. At $T = T_c$ the fast growing P_{dec} keeps up with P_{conf} and the phase transition occurs, as it is shown in Fig. 1.

One should stress the important role of V_1^{sat} , which is compensated by V_D^{sat} at $T < T_c$ (see appendix), but creates its own pair interaction $V_1(r, T)$ for $T > T_c$ [7, 43], with nonzero value at $r \rightarrow \infty$, $V_1(\infty, T)$. This term produces the Polyakov loop of gluon $L_{\text{adj}}(T) = \exp\left(-9\frac{V_1(\infty, T)}{8T}\right)$, and $L_{\text{adj}} = (L_f)^{9/4}$ increases with T and tends to constant for $T \lesssim 2T_c$. This picture was successfully confronted with lattice data in [43].

One should note at this point, that $L_{\text{adj}}(T) \equiv L_{\text{adj}}$ remains nonzero in the confined phase for $T < T_c$, where it is expressed via the gluelump mass $m_{glp} \approx 1 \text{ GeV}$, $L_{\text{adj}}^<(T) \cong \exp\left(-\frac{m_{glp}}{T}\right)$, and thus $L_{\text{adj}}(T), T < T_c$ is much smaller than $L_{\text{adj}}(T > T_c)$, in agreement with lattice data [44], as it was shown in the second refs. in [7].

However this $L_{\text{adj}}^<(T)$ does not enter the thermodynamic potential of the confined phase and its properties are not of interest for us.

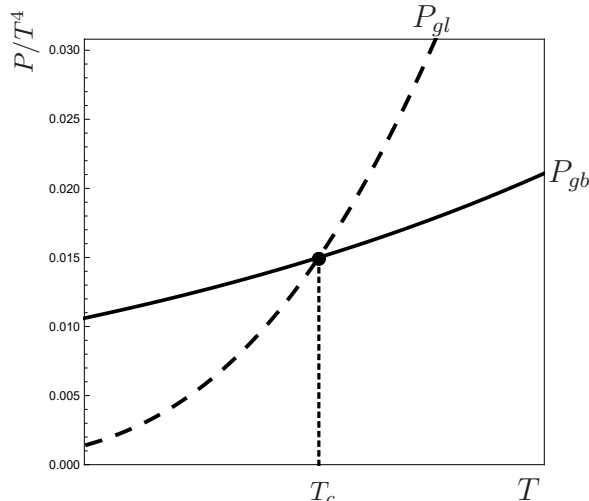


Figure 1: Pressure $P(T)$ as function of temperature T for the confined phase (glueballs) – solid line, and for the deconfined phase (dashed line). The intersection point is at the critical temperature T_c .

This general picture of the temperature dependence of FC and σ^E, σ^H is in agreement with lattice measurements of the correlators in [45], which demonstrate, that only correlator D^E vanishes at $T \geq T_c$.

Till now nothing was said about the role of the spatial string tension $\sigma_s \equiv \sigma^H$ and the magnetic confinement in general in the deconfinement transition. In the confinement region $T < T_c$, magnetic confinement is acting mostly in the hadrons with angular momentum $L > 0$, where it gives a small correction [46]. In the deconfined region the situation is different. Here closed loop trajectories of gluons and quarks for large T lie almost all in $d = 3$ space, and therefore governed by the spatial confinement growing with T . This provides every gluon with an effective mass m_{gl} proportional to $\sqrt{\sigma_s(T)}$.

The same happens with space-like gluons, exchanged by the quark or gluon currents, those acquire the np Debye mass $m_D^H \approx 2\sqrt{\sigma_s(T)}$ [47, 48]. This phenomenon lifts the IR divergences in the perturbative thermal series, noted in the well-known Linde problem [13, 14], as it is explained in a recent paper [12], see also [6] for an earlier discussion. At this point one should stress, that as found from $d = 3$ SU(3) and on the lattice [49], also within our method as shown in [12], $\sigma_s(T)$ is growing with T as $\sigma_s(T) = c_s^2 g^4(T) T^2$, and hence in our np method the CM gluon screening masses scale as $m_{gl} \sim g^2(T) T$, whereas in the perturbative theory the effective gluon mass is of the CE origin $m_D^E(T) \sim gT + O(g^2)$, where $O(g^2)$ is of the np origin.

From the practical point of view both definitions of the effective gluon mass are close numerically, since $g(T) \sim O(1)$ for $T \sim (300 - 500)$ MeV, and therefore an average gluon mass, entering in HTL [22–24] approach, may be not far from the magnetic m_D^H [47].

It is a purpose of the present paper to study the SU(3) thermodynamics in the lowest np approximation (the so-called Single-Loop Approach (SLA)) but taking into account the np correlators D_1^E and D^H for $T > T_c$, which produce Polyakov loops and σ_s respectively. We calculate from σ_s the gluon effective mass and find $P(T)$, $I(T) = \varepsilon - 3P$. We define T_c , latent heat and other characteristics and compare our results to the recent lattice measurements in [25].

The paper is organized as follows. In the next section the general field correlator

formalism for thermodynamics is shortly summarized. In section 3 the effect of magnetic confinement contributions is studied and estimated in the SLA approximation. Section 4 comprises the notion and numerical estimates of Polyakov loops, in comparison with lattice data. Section 5 is devoted to the discussion of the confinement phase and the temperature dependence of the glueball pressure, in section 6 the results of the calculation of T_c , pressure, and trace anomaly are given, while the section 7 contains a summary and perspectives.

2 General formalism

We are using the thermal background perturbation theory for the gluons in the deconfined phase II, developed in [7], where vacuum background fields are denoted by B_μ and perturbative part by a_μ . To the lowest order in ga_μ one can write for the B dependent free energy

$$\begin{aligned} \frac{1}{T} F_0^{gl}(B) &= \frac{1}{2} \ln \det G^{-1} - \ln \det(-D^2(B)) = \\ &= Sp \left\{ -\frac{1}{2} \int_0^\infty \xi(s) \frac{ds}{s} e^{-sG^{-1}} + \int_0^\infty \xi(s) \frac{ds}{s} e^{sD^2(B)} \right\}, \end{aligned} \quad (6)$$

while the vacuum averaged free energy is

$$-\frac{\langle F_0^{gl}(B) \rangle_B}{T} = \ln \left\langle \exp \left(-\frac{\langle F_0^{gl}(B) \rangle}{T} \right) \right\rangle_B. \quad (7)$$

Using the cluster expansion in the exponent

$$\begin{aligned} \langle \exp f \rangle_B &= \exp \left(\sum_{n=1}^\infty \langle \langle f^n \rangle \rangle \frac{1}{n!} \right) \\ &= \exp \{ \langle f \rangle_B + \frac{1}{2} [\langle f^2 \rangle_B - \langle f \rangle_B^2] + O(f^3) \}, \end{aligned} \quad (8)$$

one obtains the lowest order one-loop expression for $\langle F_0^{gl}(B) \rangle_B$,

$$\langle F_0^{gl}(B) \rangle_B = -T \int \frac{ds}{s} \xi(s) d^4 x (Dz)_{xx}^w e^{-K} \left[\frac{1}{2} tr \langle \tilde{\Phi}_F(x, x) \rangle_B - \langle tr \tilde{\Phi}(x, x) \rangle_B \right]. \quad (9)$$

Here the winding path integration is

$$\begin{aligned} (Dz)_{xy}^w &= \lim_{N \rightarrow \infty} \prod_{m=1}^N \frac{d^4 \zeta(m)}{(4\pi\varepsilon)^2} \\ &\sum_{n=0, \pm, \dots} \frac{d^4 p}{(2\pi)^4} \exp \left[ip_\mu \left(\sum_{m=1}^N \zeta_\mu(m) - (x-y)_\mu - n\beta\delta_{\mu 4} \right) \right]. \end{aligned} \quad (10)$$

and $\tilde{\Phi}(x, x)$ is the adjoint parallel transporter

$$\tilde{\Phi}(x, y) = P \exp \left(ig \int_y^x \tilde{B}_\mu dz_\mu \right), \quad (11)$$

while $\tilde{\Phi}_F$ contains additional gluon spin factor, $P_F \exp(2ig \int_0^s \tilde{F} d\tau)$, which we shall replace by unity in the lowest approximation¹. As a result the gluon pressure $P_{gl} V_3 = -\langle F_0^{gl}(B) \rangle_B$ can be written as

$$P_{gl} = (N_c^2 - 1) \int_0^\infty \frac{ds}{s} \sum_{n=0, \pm 1, \pm 2, \dots} G^{(n)}(s). \quad (12)$$

$G^{(n)}$ in (12) is defined as

$$G^{(n)}(s) = \int (Dz)_{on}^w e^{-K} \langle \hat{tr}_a W(C_n) \rangle, \quad (13)$$

where

$$K = \frac{1}{4} \int_0^s \left(\frac{dz_\mu(\tau)}{d\tau} \right)^2 d\tau, \quad (14)$$

$$\langle \hat{tr}_a W(C_n) \rangle = \frac{tr_a}{(N_c^2 - 1)} \langle \tilde{\Phi}(x, x^{(n)}) \rangle. \quad (15)$$

Note here, that the generic path of the gluon starts at the point x and ends at the point $x^{(n)} = x_\mu + n\beta \cdot \delta_{\mu 4}$, as shown in (10), so that one has a closed loop in 3d, while the projection on the 4-th axis yields the Polyakov loop, L_{adj} . Indeed, for the propagator $G(x, y)$ the Matsubara assignment in (10) yields a sum of end points $y_4^{(n)} = y_4 + n\beta, n = 0, \pm 1, \dots$ which for the coinciding $x_4 = y_4$ results in an infinitive series of open contours $[y_4, y_4 + n\beta]$, with the unitary gauge equivalent points $U(y_4 + n\beta) = U(y_4)$. Now multiplying the contours with the product of gauge invariant lines (11), $\tilde{\Phi}(y_4, y_4 + n\beta) \times \tilde{\Phi}(y_4 + n\beta, y_4) = 1$, and taking the vacuum average, one obtains the product of the closed Wilson loop W_3 and the Polyakov line $L_{adj}(T)$ (modulo insignificant correlation between the CE contents of L_{adj} and CM of W_3).

As a result (15) can be written as

$$\frac{tr_a}{(N_c^2 - 1)} \langle \tilde{\Phi}(x, x^{(n)}) \rangle = L_{adj}^{(n)}(T) \langle W_3 \rangle, \quad (16)$$

where $\langle W_3 \rangle$ is the spatial area law factor

$$\langle W_3 \rangle = \exp(-\sigma_s A_3) \quad (17)$$

and A_3 is the minimal area in the 3d space of the loop, formed by trajectories $z_i(\tau), 0 \leq \tau \leq s, i = 1, 2, 3$.

It will be essential that $\sigma_s(T)$ grows with T as [12, 49]

$$\sigma_s(T) = c_\sigma^2 g^4(T) T^2, \quad (18)$$

where c_σ is a dimensionless constant defined in a np way. The form (18) was found on the lattice [49] with $c_\sigma = 0.566 \pm 0.013$. The similar form was found in $d = 4$ [12, 48], using the gluelump Green's function method [36, 37]. For $T < T_c$, σ_s tends to a constant $\sigma_s = \sigma^{(E)}$.

We turn now to the first factor on the r.h.s. of (16). As it is shown in [7], for $T > T_c$ one can express $L_{adj}^{(n)}$ via the CE correlator $D_1^E(z)$,

$$L_{adj}^{(n)} = \exp\left(-\frac{9}{4} J_n^E\right), \quad J_n^E = \frac{n\beta}{2} \int_0^{n\beta} d\nu \left(1 - \frac{\nu}{n\beta}\right) \int_0^\infty \xi d\xi D_1^E(\sqrt{\xi^2 + \nu^2}) \quad (19)$$

¹ Here P, P_F are ordering operators for the fields \tilde{B}_μ and $\tilde{F}_{\mu\nu}$ respectively

It is argued in [7], that a good approximation for $T < 1$ GeV is $J_n^E \cong nJ_1^E$, which we shall use in what follows.

The integral $(Dz_4)_{on}^w$ in (13) for $T > T_c$ can be done explicitly, yielding [7]

$$G^{(n)}(s) = \frac{1}{\sqrt{4\pi s}} e^{-\frac{n^2}{4T^2 s}} G_3(s) L_{\text{adj}}^{(n)}, \quad (20)$$

where $G_3(s)$ is

$$G_3(s) = \int (D^3 z)_{xx} e^{-K_{3d}} \langle W_3 \rangle, \quad (21)$$

and as a result the gluon pressure in the phase II has the form

$$P_{gl} = \frac{N_c^2 - 1}{\sqrt{4\pi}} \int_0^\infty \frac{ds}{s^{3/2}} G_3(s) \sum_{n=0,1,2,\dots} e^{-\frac{n^2}{4T^2 s}} L_{\text{adj}}^{(n)}. \quad (22)$$

$$F_{gl} = -P_{gl} V_3, \quad (23)$$

3 Calculation of the spatial loop

We consider here $G_3(s)$, Eq.(21), which corresponds to the 3d loop, which is governed by the spatial confinement with the string tension $\sigma_s(T)$. It is clear, that gluons on the opposite sides of the loop are connected by the confining string, and we transform the integral (21) to make it explicit. To this end we write the identity

$$(D^3 z)_{xx} = (D^3 z)_{xu} d^3 u (D^3 z)_{ux}, \quad (24)$$

where we choose the point u_i as $u_i = z_i \left(\frac{s}{2} \right)$.

Using $u_3 \equiv t$ as the Euclidean time in 3d, one can write

$$(Dz_3)_{x_3 u_3} e^{-K_3} = \frac{1}{\sqrt{2\pi s}}, \quad K_3 = \frac{1}{4} \int_0^{s/2} \left(\frac{dz_3}{d\tau} \right)^2 d\tau. \quad (25)$$

As a result $G_3(s)$ acquires the form

$$G_3(s) = \int (D^2 z)_{xu} d^2 u (D^2 z)_{ux} e^{-K_1 - K_2} \langle W_3 \rangle \frac{dt}{2\pi s}. \quad (26)$$

Using (17) one can express $\langle W_3 \rangle$ in terms of the instantaneous confining potential $V_{\text{conf}} = \sigma_s |\mathbf{r}_1 - \mathbf{r}_2|$, $\langle W_3 \rangle = \exp(-V_{\text{conf}} t)$.

One can write K_1, K_2 as follows

$$K_1 + K_2 = \frac{1}{4} \sum_{i=1,2} \int_0^{s_i} d\tau_i \left(\frac{d\mathbf{z}^{(i)}}{d\tau} \right)^2 \quad (27)$$

and introducing ω_i instead of s_i , $s_i = \frac{t}{2\omega_i}$ one obtains in the exponent

$$K_1 + K_2 + V_{\text{conf}}(\eta)t \rightarrow \left(\frac{\mathbf{p}_1^2}{2\omega_1} + \frac{\mathbf{p}_2^2}{2\omega_2} + \frac{\omega_1 + \omega_2}{2} + V_{\text{conf}}(\eta) \right) t, \quad (28)$$

where $\eta = |\mathbf{z}^{(1)} - \mathbf{z}^{(2)}|$. On the other hand one can introduce the unit operator

$$1 = 2 \int ds_1 ds_2 \delta(s_1 + s_2 - s) \delta(s_1 - s_2) = \int \frac{td\omega_1}{\omega_1^2} \delta\left(\frac{t}{\omega_1} - s\right) d\omega_2 \delta(\omega_2 - \omega_1) = \frac{td\omega}{\omega^2} \delta\left(\frac{t}{\omega} - s\right). \quad (29)$$

Using Eq. (17) in [?] one can rewrite (26) with (29) as

$$G_3(s) = \int \frac{tdtd\omega}{2\pi s\omega^2} \delta\left(\frac{t}{\omega} - s\right) d^2u \langle xx | e^{-H(\mathbf{P})t} | uu \rangle, \quad (30)$$

where

$$H(P) = \frac{\mathbf{P}^2}{4\omega} + \frac{\mathbf{p}^2}{\omega} + \omega + V_{\text{conf}}, \quad (31)$$

and finally, integrating out the free center-of-mass coordinate

$$\int d^2u \langle xx | e^{-H(\mathbf{P})t} | uu \rangle = \int d^2u \frac{d^2\mathbf{P}}{(2\pi)^2} e^{i\mathbf{P}(\mathbf{x}-\mathbf{u})} \langle 0 | e^{-H(\mathbf{P})t} | 0 \rangle = \langle 0 | e^{-H(0)t} | 0 \rangle, \quad (32)$$

where in $\langle 0 |, | 0 \rangle$, enter only w.f. of relative motion.

The eigenvalues of $H(0)$ can be found in the same way, as it was done in [15], using the local limit of $H(0)$ in ω at $\omega = \omega_0$,

$$M = 4\omega_\nu^{(0)}; \quad \omega_\nu^{(0)} = \left(\frac{a_\nu}{3}\right)^{3/4} \sqrt{\sigma_{\text{adj}}}, \quad \sigma_{\text{adj}} = \frac{9}{4}\sigma_s, \quad a_0 = 1.74, \quad (33)$$

which yields the lowest eigenvalues

$$\omega_0^{(0)} \approx \sqrt{\sigma_s}, \quad M_0 = 4\sqrt{\sigma_s}.$$

Finally one obtains

$$G_3(s) = \frac{1}{\sqrt{\pi s}} \sum_{\nu=0,1,\dots} \psi_\nu^2(0) e^{-M_\nu \omega_\nu^{(0)} s} \quad (34)$$

and $\psi_\nu^2(0) = c_\nu \sigma_s$, where the dimensionless constant c_ν has to be defined, solving the wave equation with the Hamiltonian $H(0)$.

Hence the lowest mass squared in (34) is

$$\mu_0^2 = M_0 \omega_0^{(0)} \cong 4\sigma_s \approx m_D^2, \quad (35)$$

where m_D is the screening mass found in [47]. One can check the general expression (34) in the free case, $\sigma_s \equiv 0$. In this case $\sum_n \psi_n^2(0) = \frac{d^2 p}{(2\pi)^2}$ and $M_n, \omega_n^{(0)}$ from $H_0 = \frac{\mathbf{P}^2}{\omega} + \omega$, Eq. (31), are $\omega_0 = |\mathbf{p}|, M_0 = 2p$ and one obtains the exact free result.

$$G_3^{(0)}(s) = \frac{1}{\sqrt{\pi s}} \int \frac{d^2 p}{(2\pi)^2} e^{-2p^2 s} = \frac{1}{\sqrt{\pi s}} \frac{1}{8\pi s} = \frac{1}{(4\pi s)^{3/2}}, \quad (36)$$

which using (20) and (12) yields the Stefan-Boltzmann result ($L_{\text{adj}} \equiv 1$)

$$P_{gl}^{(0)} = \frac{N_c^2 - 1}{(4\pi)^2} \int_0^\infty \frac{ds}{s^3} \sum_{n=\pm 1, \pm 2} e^{-\frac{n^2}{4T^2 s}} = \frac{2(N_c^2 - 1)T^4}{\pi^2} \sum_{n=1}^\infty \frac{1}{n^4} = \frac{(N_c^2 - 1)T^4 \pi^2}{45}. \quad (37)$$

Using (34) one can write $P_{gl}^{(1)}$ as (keeping the only term with $\nu = 0$, $\psi_0^2(0) \equiv \bar{c}\sigma_s$)

$$P_{gl}^{(1)} = \frac{N_c^2 - 1}{(4\pi)^2} \int_0^\infty \frac{ds}{s^2} \bar{c}\sigma_s e^{-m_D^2(T)s} \sum_{n=\pm 1, \pm 2} e^{-\frac{n^2}{4T^2 s}} L_{\text{adj}}^{(n)}. \quad (38)$$

From the integral representation of the modified Bessel function

$$K_\nu(z) = \frac{1}{2} \left(\frac{z}{2}\right)^\nu \int_0^\infty \frac{e^{-t - \frac{z^2}{4t}}}{t^{\nu+1}} dt, \quad (39)$$

one arrives at the following form (taking into account, that $L_{\text{adj}}^{(n)} \approx (L_{\text{adj}})^n$ for $T \lesssim \lambda^{-1} = 1$ GeV, as it is shown in [7])

$$P_{gl}^{(1)}(T) = \frac{(N_c^2 - 1)\bar{c}\sigma_s m_D T}{2\pi^2} \sum_{n=1,2,\dots} \frac{1}{n} K_1\left(\frac{nm_D}{T}\right) (L_{\text{adj}})^n. \quad (40)$$

On the other hand one can use the relation

$$\sum_{n=1,2,\dots} \frac{K_\nu(nz)}{n^\nu} = \frac{\sqrt{\pi}}{\Gamma(\nu + \frac{1}{2}) (2z)^\nu} \int_0^\infty \frac{t^{2\nu} dt}{\sqrt{t^2 + z^2} (\exp(\sqrt{t^2 + z^2}) - 1)}, \quad (41)$$

and one obtains

$$P_{gl}^{(1)}(T) = \frac{(N_c^2 - 1)\bar{c}\sigma_s T^2}{2\pi^2} \int_0^\infty \frac{t^2 dt}{\sqrt{t^2 + \left(\frac{m_D}{T}\right)^2}} \frac{1}{\exp\left(\sqrt{t^2 + \left(\frac{m_D}{T}\right)^2} + a\right) - 1}, \quad (42)$$

$L_{\text{adj}} = \exp(-a)$.

Note, that we have kept the lowest eigenvalue $\nu = 0$ in (34), in a more general case one should replace $\bar{c} \rightarrow \bar{c}_\nu$, $m_D \rightarrow m_D^{(\nu)}$ and sum over ν , $\nu = 0, 1, 2, \dots$. However, having in mind, that $m_D^{(\nu)}$ strongly rise in magnitude with growing ν , and they enter in the exponent in (42), one can expect that the first term with $\nu = 0$ yields a reasonable approximation for not large T . In what follows we keep the form (42) with \bar{c} being a free constant, to be fixed by comparison with lattice data at some point of T .

One can simplify the answer in the case, when the spatial confinement has the form of an oscillator potential. In this case one can write $G^{(n)}(s)$ in (14) as

$$G^{(n)}(s) = \int (Dz_4)_{0n}^w (Dz_3)_{00} (Dz_1)_{00} (Dz_2)_{00} e^{-K} = \frac{1}{4\pi s} e^{-\frac{n^2}{4T^2 s}} G_2(0, 0, s), \quad (43)$$

$$G_2(0, 0, s) = \int (Dz_1)_{00} (Dz_2)_{00} e^{-K_1 - K_2} = \frac{M_0^2}{4\pi \text{sh} M_0^2 s}. \quad (44)$$

Here $M_0 = \omega$ is the lowest mass (excitation) in the oscillator potential, which we might associate with the lowest screening mass m_D .

As a result one obtains the gluon pressure in the form

$$P_{gl}^{(OCS)} = \frac{2(N_c^2 - 1)}{(4\pi)^2} \sum_{n=1}^{\infty} L_{adj}^{(n)} \int_0^{\infty} \frac{ds}{s^2} e^{-\frac{n^2}{4T^2}s} \frac{M_0^2}{\text{sh} M_0^2 s}. \quad (45)$$

One can check, that for $M_0 \ll T$ (45) yields the Stefan-Boltzmann result (37), augmented by the term L^n .

To make a connection with the realistic case of linear confinement, $V(r) = \sigma_s r$, one can make a substitution $\sigma_s r \rightarrow \frac{\sigma_s}{2} \left(\frac{r^2}{\gamma} + \gamma \right)$, which after variation in the parameter γ yields back the linear potential. The use of this trick was checked to give approximately 5% accuracy in the spectrum calculations. As a result one obtains a crude approximation for $G_3(s)$, Eq. (21) of the linear potential

$$G_3^{\text{lin}}(s) \rightarrow \frac{1}{2}(\gamma G_3^{(0)}(s) + \frac{1}{\gamma} G_3^{(OSC)}(s)) \rightarrow \frac{1}{(4\pi s)^{3/2}} \sqrt{\frac{M_0^2 s}{\text{sh} M_0^2 s}} \quad (46)$$

and as a result one obtains

$$P_{gl} = \frac{2(N_c^2 - 1)}{(4\pi)^2} \sum_{n=1}^{\infty} L_{adj}^{(n)} \int_0^{\infty} \frac{ds}{s^3} e^{-\frac{n^2}{4T^2}s} \sqrt{\frac{M_0^2 s}{\text{sh} M_0^2 s}}. \quad (47)$$

In what follows we shall use (47) with $M_0 \approx m_D$, and we shall find that the results of (45) and (47) are rather close numerically.

4 Polyakov lines in the Field correlator approach

As was discussed in the Introduction, the CE gluon correlators produce the potential $V_1^{\text{sat}}(r) = V_1(\infty) + v(r)$, Eq. (4), so that in the gg Green's function acquires the factor $\Lambda \equiv \exp\left(-c_a \frac{V_1(\infty)}{2} t_4\right)$ for each gluon, when one considers $v(r)$ as a perturbation.

However, in the confined region V_1^{sat} is screened by the $V_D(r, T)$, and therefore this factor Λ appears only in the deconfined phase, where it appears in the form of the Polyakov line.

In the Matsubara representation of the temperature Green's function $G^{(n)}(s)$, Eq. (13), one has the phase J_n^E , Eq. (19) which tends to $\frac{nV_1(\infty)}{2T}$ for $T \rightarrow 0$, in agreement with Λ , when $t_4 = 1/T$.

Thus Eq. (19) defines the Polyakov loop at $T > 0$ and also at $T > T_c$ via $V_1(r, T)$, namely

$$L_{\text{adj}}^{(n)} = \exp\left(-\frac{9n}{8T} V_1^{(n)}(\infty, T)\right). \quad (48)$$

$$V_1^{(n)}(\infty, T) = \int_0^{n/T} d\nu \left(1 - \frac{\nu T}{n}\right) \int_0^{\infty} \xi d\xi D_1^E\left(\sqrt{\xi^2 + \nu^2}\right). \quad (49)$$

The important property to be used in what follows, is the short distance behavior of $D_1^E(x)$, which is concentrated at distances $|x| \lesssim \lambda = 0.2$ fm and is assumingly not affected by T for $T < 1/\lambda \cong 1$ GeV [37, 43, 48]. In this case one can make a replacement,

$n \rightarrow 1$ in (49), and omit the superscript n in $V_1^{(n)}(r, T)$, as we shall do in what follows writing

$$L_{\text{adj}}^{(n)} = (L_{\text{adj}}(T))^n, \quad L_{\text{adj}}(T) = \exp\left(-\frac{9V_1(\infty, T)}{8T}\right), \quad (50)$$

where $V_1(\infty, T)$ is given in (49) via the correlator $D_1^E(x)$.

Note two important consequences of our theory for $L(T)$: first of all the $Z(3)$ symmetry of the $SU(3)$ theory is spontaneously broken by the vacuum field correlator, which fixes one of 3 branches with $N = 0$.

Secondly, the Casimir scaling for $L_J(T)$ observed on the lattice [44], appears naturally, since $V_1^{(a)}(T)$ is proportional to c_a .

To compute $P(T)$, $I(T)$ etc. numerically we need the explicit form of $V_1(\infty, T)$ or $D_1(x - y)$. In the phase II for $T < T_c$ this can be derived, using the gluelump Green's functions and eigenvalues [37]. Using the same form also for $T > T_c$ it was found in [43], that the function $V_1(\infty, T)$, agrees approximately with the lattice free energy $F_1(\infty, T)$ [50]. In what follows we shall use this form, however we shall take into account that on general grounds $F_1(\infty, T) < V_1(\infty, T)$ and the negative values of $F_1(\infty, T)$ for large $T \gg T_c$ do not provide negative $V_1(\infty, T)$ and hence $L(T) \leq 1$ [43]. One can also argue, that our $L(T) < L_{\text{lat}}(T)$.

The Polyakov line can also be obtained from the gluelump form of the correlator D_1 , which can be written according to [43] as

$$D_1^{(np)}(x) = \frac{A_1}{|x|} e^{-M_1|x|} + O(\alpha_s^2), \quad A_1 = 2C_2\alpha_s\sigma_{\text{adj}}M_1, \quad x \geq 1/M_1. \quad (51)$$

and the nonperturbative part of V_1 (note that D_1 contains also the perturbative gluon exchange correlator), which for $T = 0$ has the form (2), for $T > 0$ can be written as

$$V_1^{(np)}(r, T) = A_1 \int_0^{1/T} (1 - \nu T) d\nu \int_0^r \frac{\xi d\xi e^{-M_1\sqrt{\xi^2 + \nu^2}}}{\sqrt{\xi^2 + \nu^2}}, \quad (52)$$

which yields at $r \rightarrow \infty$

$$L_f = \exp\left(-\frac{V_1^{(np)}(\infty)}{2T}\right), \quad V_1^{(np)}(\infty) = \frac{A_1}{M_1^2} \left[1 - \frac{T}{M_1}(1 - e^{-M_1/T})\right]. \quad (53)$$

One can also use directly its lattice renormalized values, and we shall prefer the $L^{\text{ren}}(T)$ from [44], where $L_a^{\text{ren}}(T)$ were found for different $SU(3)$ representations a , and the Casimir scaling was established with good accuracy.

The comparison of $L_{\text{adj}}(T)$ in the region $T > T_c$ with the lattice data [44] in Fig. 2 shows a reasonable agreement.

One can compare (52), (53) with the lattice data for the pair free energy F_1 [50], which yields for $V_1(\infty, T)$ the value $V_1(\infty, T_c) \approx 0.5$ GeV (with 10% accuracy) and decreasing with growing T , and we approximate $V_1^F(\infty, T)$ as obtained from F_1

$$V_1^F(\infty, T) = \frac{0.175 \text{ GeV}}{1.35 \frac{T}{T_c} - 1}, \quad T \geq T_c \quad (54)$$

At this point one should stress, as it was also done in [43] the difference between $V_1(r, T)$ and $F_1(r, T)$, measured on the lattice, which can be written as

$$e^{-F_1(r, T)/T} = \sum_n e^{-E_n(r, t)/T}, \quad (55)$$

and $E_0(r, T)$ can be associated with $V_1(r, T)$, while higher in n states make F_1 smaller than V_1 , and finally can make it negative at larger T , as it was found on the lattice.

To account for the difference V_1 and F_1 we can use another form $V_1^{(\text{mod})}(\infty, T)$, where $V_1^{(\text{mod})} > F_1$, namely

$$V_1^{(\text{mod})}(\infty, T) = \frac{0.13 \text{ GeV}}{T/T_c - 0.84}. \quad (56)$$

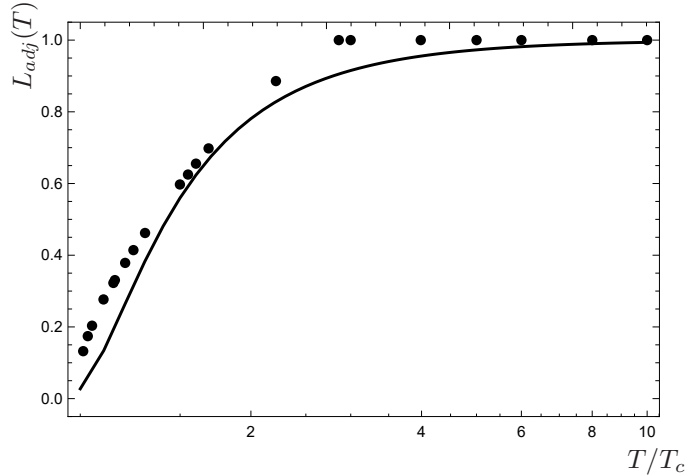


Figure 2: Polyakov line $L_{\text{adj}}(T)$: the solid line is our modified $L_{\text{adj}}^{(\text{mod})}(T)$ from Eqs. (56),(57) and filled dots are for the lattice data [44].

In Fig. 2 we show both the lattice data for $L_{\text{adj}}(T)$ taken from [44] and our modified $L_{\text{adj}}^{(\text{mod})}(T)$, calculated as

$$L_{\text{adj}}^{(\text{mod})}(T) = \exp \left(-\frac{9V_1^{(\text{mod})}(\infty, T)}{8T} \right). \quad (57)$$

One can see a reasonable agreement between two lines, satisfying the required relation $L_{\text{adj}}^{(\text{mod})}(T) \lesssim L_{\text{adj}}^{\text{lat}}(T)$. The form (57) is used below in our calculations of all thermodynamic functions.

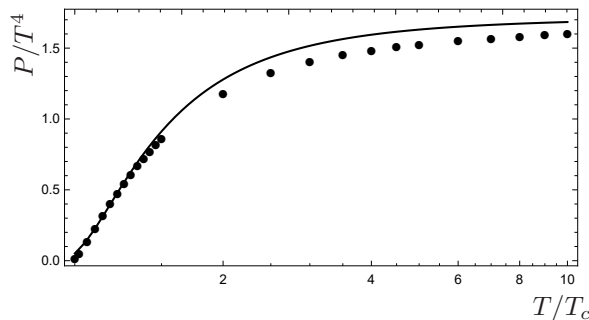


Figure 3: The pressure $P(T)/T^4$ in the $SU(3)$ theory in the deconfined phase. The solid line is for the modified oscillator confinement Eq. (47), and filled dots are for the lattice data [25].

The resulting pressure $P_{gl}(T)$ for $T \geq T_c$ is shown in Fig. 3. One can see, that the use of $L_{\text{adj}}^{(\text{mod})}(T)$ from (57), (56) and of the magnetic confinement, Eq. (47) gives a reasonable agreement with lattice $SU(3)$ data from [25].

5 The confinement sector

We now turn to the confined gluonic phase, which consists of the two-gluon, three-gluon, etc. glueballs, which can be calculated analytically via $\sigma^{(E)}$ [51]. The corresponding pressure of the noninteracting gas of glueballs of the i -th kind with mass m_i is [52]

$$P_{gb}^{(i)} = \frac{g_i T^2}{2\pi^2} \sum_{n=1}^{\infty} \frac{m_i^2}{n^2} K_2\left(\frac{nm_i}{T}\right), \quad (58)$$

where g_i is the multiplicity of the i -th glueballs.

We have disregarded in (58) the contribution of the possible real or virtual glueball decay products, as well as the interaction between glueballs, which disappears in the large N_c limit.

The total pressure, P_{conf} , in the SU(3) case is given by the sum of the glueball terms (58), namely

$$P_{\text{conf}} = \sum_i P_{gb}^{(i)}. \quad (59)$$

The situation here depends on the spectrum of lowest glueballs, which was found repeatedly on the lattice [53–55] and also analytically in the Field Correlator Method [51], see comparison in the Table 1, which shows a remarkable agreement of almost all states. One expects that, the total contribution of the excited glueballs might be important in the region near T_c , and the question arises, how one approximates the asymptotic behavior of the spectrum.

A most detailed lattice analysis of the SU(3) thermodynamics done recently in [25], reveals that e.g. the trace anomaly below and near T_c can be described by a combination of glueball and Hagedorn contributions [56] (see Figs. 3 and 4 in [25]).

In an accurate analysis of the entropy density s in [57] it was found, that 0^{++} and 2^{++} glueballs contribute to s/T^3 less than 25% at $T = T_c$, and only the combination of glueballs with mass less than $2M_0$ (two-particle threshold) and the Hagedorn spectrum corresponds to the lattice data.

However, from our point of view the use of the Hagedorn density of states [56], derived from the closed string spectrum, in addition to the 10-12 lowest glueballs, seems to be superfluous. Indeed, there is no evidence that the Hagedorn spectrum has quantitative correspondence with the realistic glueball spectrum, and that the closed strings are resemblant to multigluon glueball states. One can also add, that strictly speaking the 4d string theory does not exist.

Moreover, it is hard to imagine, that high excited closed string states are realized on the finite size lattice.

Therefore we turn to another explanation of the high growing glueball contribution to P_{conf} near T_c . Namely, it was repeatedly found on the lattice (see e.g. [40], [41] and [42]), that the string tension σ_E starts to depend on T in the region $0.7T_c \leq T \leq T_c$, and tends to a value $\sigma_E(T_c)$, which is in the region $0.2\sigma_0 \leq \sigma_E(T_c) \leq 0.5\sigma_0$. here $\sigma_0 = \sigma_E(T = 0)$. It is clear physically, that glueball masses decrease as $m_i(T) = a(T)m_i(0)$, where $a(T) = \sqrt{\frac{\sigma_E(T)}{\sigma_0}}$.

As a result in (58) one obtains a strong amplification of the glueball pressure. Indeed, writing $a(T)$ as

$$a(T) = \sqrt{1 - \left(\frac{T}{T_c + b}\right)^2} \quad (60)$$

one obtains the pressure P_{conf} in (59) for 12 and 2 lowest glueballs, shown in Fig. 4.

Table 1: Glueball masses from FCM as compared to lattice data

J^{PC}	$M(\text{GeV})$	Lattice data		
	Ref. [41]	Ref. [51]	Ref. [52]	Ref. [53]
0^{++}	1.58	1.710(50)(80)	1.73 ± 0.13	1.74 ± 0.05
0^{++*}	2.71		2.67 ± 0.31	3.14 ± 0.10
2^{++}	2.59	2.39	2.40 ± 0.13	2.47 ± 0.08
2^{++*}	3.73		3.29 ± 0.16	3.21 ± 0.35
0^{-+}	2.56	2.56	2.59 ± 0.17	2.37 ± 0.27
0^{-+*}	3.77		3.64 ± 0.24	
2^{-+}	3.03	3.04	3.1 ± 0.18	3.37 ± 0.31
2^{-+*}	4.15		3.89 ± 0.23	
3^{++}	3.58	3.67	3.69 ± 0.22	4.3 ± 0.34
1^{--}	3.49	3.83	3.85 ± 0.24	
2^{--}	3.71	4.01	3.93 ± 0.23	
3^{--}	4.03	4.20	4.13 ± 0.29	

One can see in Fig. 4 the resulting $P_{\text{conf}}(T)$ as a function of T in comparison with the lattice data [25] for two cases: 1) when only 0^{++} and 2^{++} glueballs are retained, and 2), when 12 lowest glueball states are included with $a(T)$ (60) and $b = 0.15 T_c$. One can see a good agreement of $P_{\text{conf}}(T)$ in the case 2) with the lattice data from [25] for the chosen value of b . At the same time we present in Fig. 5 the comparison of our resulting behavior of $\frac{\sigma(T)}{\sigma_0}$ with the lattice measurements of confinement attenuation in [40–42], which shows a reasonable qualitative agreement.

Thus we conclude, that there is no need to exploit the Hagedorn mechanism for the explanation of the pressure P_{conf} near T_c .

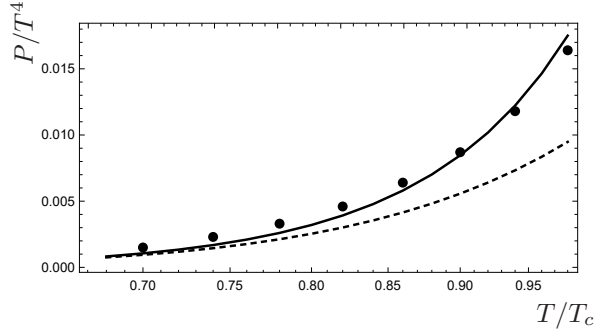


Figure 4: Pressure in the confining phase. The dashed line is for 2 lowest glueballs (0^{++} and 2^{++}) and the solid line is for 12 glueballs. The filled dots are for the lattice data [25].

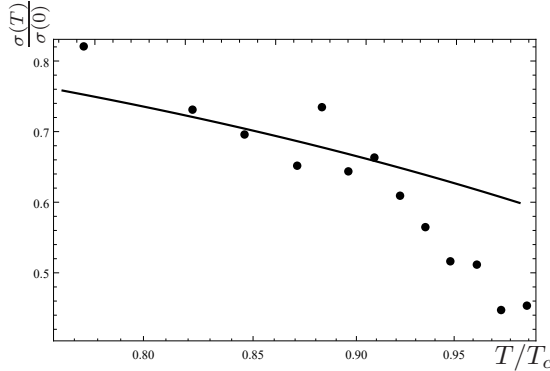


Figure 5: The solid line is for the string tension $\sigma(T)/\sigma(0)$ calculated from Eq. (60), and dots are for the lattice data [41].

6 Results for the SU(3) phase transition and trace anomaly

In this section we combine together our results for the confined and deconfined phases. In doing so we calculate also the trace anomaly $\frac{I(T)}{T^4} = \frac{\varepsilon - 3P}{T^4}$, and the entropy density $s(T) = \left(\frac{dP(T)}{dT}\right) \frac{1}{T^3}$.

We calculate $P_{gl}(T)$, as in (47) with the account of the Polyakov loops $L_{adj}(T)$, given in (56), (57) and the colormagnetic confinement as in (47). The comparison of our $P_{gl}(T)$ and the corresponding lattice values from [25] in Fig. 3 shows a good agreement in the interval $T_c \leq T \leq 10 T_c$. For P_{conf} eqs. (58) and (59) are used with masses $m_i(T) = a(T)m_i(0)$, where $a(T)$ is given in (60) and masses $m_i(0)$ in Table 1, the first column.

In P_{conf} we distinguish two cases with number of glueballs equal to a) 2 and b) 12, and $a(T)$ given in (60). These analytic results are shown in Fig. 4 in comparison with lattice data from [25].

We are using the phase transition condition, which can be written as

$$P_{gl}(T_c) = P_{conf}(T_c), \quad (61)$$

which yields $T_c \simeq 260$ MeV, as shown in Fig. 6. This agrees with lattice data from [16–19] and [25].

An important measure of the interaction is the trace anomaly, which we compute analytically as $I(T) = \varepsilon - 3p$ both below T_c in Fig. 7 and above T_c in Fig. 8. The results for $\frac{I(T)}{T^4}$ are compared with the lattice data from [25] and demonstrate a good agreement.

As a next step we find $I_{<}(T_c)$ from the confinement phase and $I_{>}(T_c)$ for the deconfined phase and calculate the difference $\frac{\Delta I(T_c)}{T^4} = \frac{I_{>}(T_c)}{T^4} - \frac{I_{<}(T_c)}{T^4}$, which for $T_c = 0.260$ GeV is equal to $\frac{\Delta I(T_c)}{T^4} = 0.61$, while $\frac{\Delta \varepsilon(T_c)}{T^4} = 0.66$.

One can compare this value with the lattice data from [58], $\frac{\Delta(\varepsilon - 3P)}{T_c^4} = 0.6223 \pm 0.056$, while in [57] it was obtained $\frac{\Delta(\varepsilon - 3P)}{T_c^4} = 1.39(4)(5)$. This latter value is close to the measured in [16] and [59].

We now turn to the behavior of $I(T)$ for $T > T_c$, where the lattice data [25] discovered an interesting shoulder in the dependence of $\frac{I(T)}{T^2 T_c^2}$ in the range $T_c \leq T \leq 4T_c$.

It was shown in our previous work [60], that this is of purely np origin and is provided by $1/T^2$ behavior of $L(T)$. One can see our analytic results in reasonable agreement with

the lattice data for $\frac{I(T)}{T^4}$ and $\frac{I(T)}{T^2 T_c^2}$ in Figs. 8, 9.

Finally in Fig. 10 we show the entropy density $\frac{s(T)}{T^3}$, which agrees with lattice data from [25].

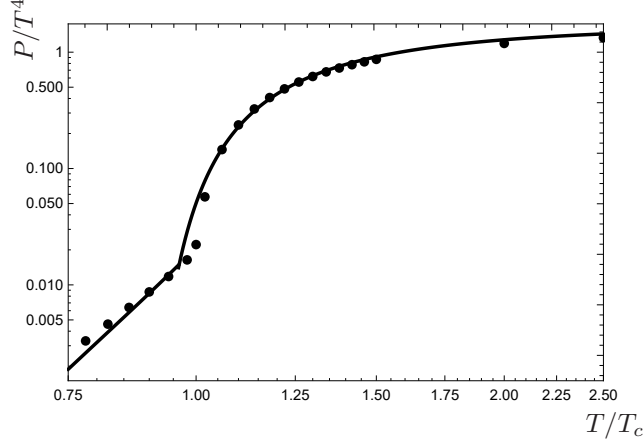


Figure 6: The pressure of the $SU(3)$ theory in the confining and deconfining phases. Filled dots are for the lattice data [25].

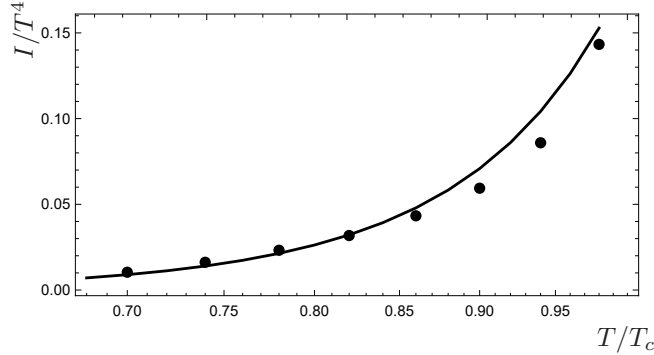


Figure 7: The trace anomaly in the confined phase, filled dots are for the lattice data [25].

7 Discussion of results and conclusions

In this paper, as well as in our previous paper [60], we have used the standard definition of the pressure $P(T)$ and other thermodynamic characteristics, both below and above T_c , without including in $P(T)$ vacuum contributions $\Delta\epsilon_{vac}V_3$, as it was done in the previous papers [5–9]. This has allowed us to make a direct comparison of our analytic and numerical results with other approaches and first of all, with the numerical results of lattice calculations. The accurate lattice data of [25] for $P(T)$, $I(T)$ and $s(T)$ have been used to compare with our results, which demonstrates a satisfactory to a good agreement between the corresponding data.

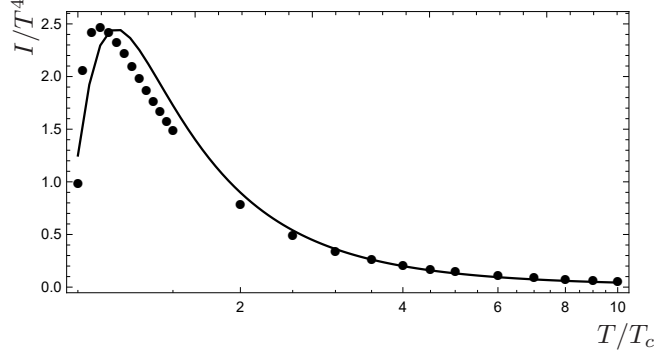


Figure 8: The trace anomaly in the deconfined phase, filled dots are for the lattice data [25].

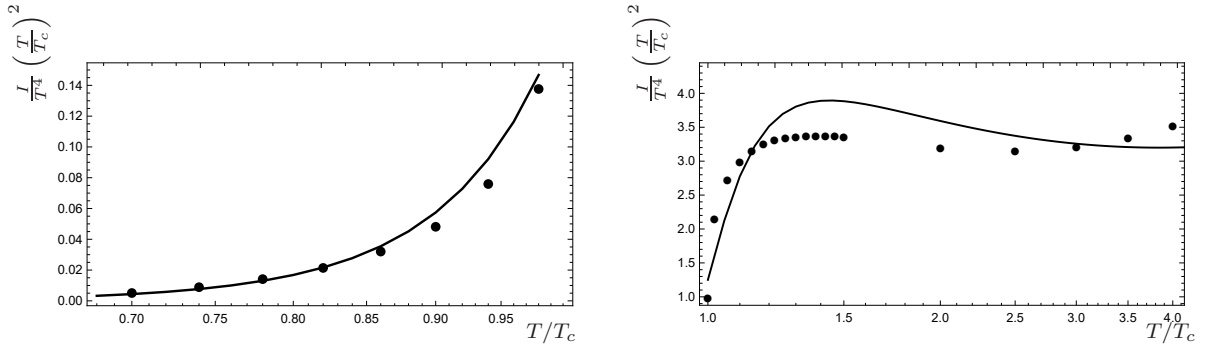


Figure 9: The trace anomaly multiplied by $(T/T_c)^2$ in the confined phase — the left panel, and in the deconfined phase — the right panel. The filled dots are for the lattice data [25].

We have kept in the present paper the same approach, as in previous ones, of the explicit definition of two phases with two different dynamics: the confined phase with CE and CM confinement and correlators, and the suppressed Polyakov lines, and the deconfined phase with CM confinement and correlators and resurrected Polyakov lines.

We have used confining interaction, derived and checked numerously to calculate lowest glueball masses in good agreement with lattice data, to calculate $P_{\text{conf}}(T)$. In doing so, we have applied the variable vacuum principle, allowing to suppress vacuum contribution to the dynamics (e.g. the string tension $\sigma(T)$), if it results in the increasing of $P(T)$.

In this way $\sigma(T)$ decreases for $T \gtrsim 0.7T_c$, making the glueball masses lighter and enhancing $P(T)$ in good agreement with numerical lattice data from [25].

The effect of the temperature dependence of the string tension $\sigma(T)$ is well known from numerous lattice measurements, see e.g. [40–42], which support the principle mentioned above.

The comparison of our curves for $\sigma(T)$ with the lattice data from [40–42] in Fig. 5 shows a qualitative agreement.

This point has allowed to avoid the use of the popular Hagedorn fitting, which is not well founded in our case, as we stressed above. Moreover, the latter is not exploited in the case of $n_f > 0$.

However our form of the string tension quenching, Eq.(58) is still the fitting procedure. It agrees qualitatively with the lattice data, as shown in Fig. 5, but should be derived

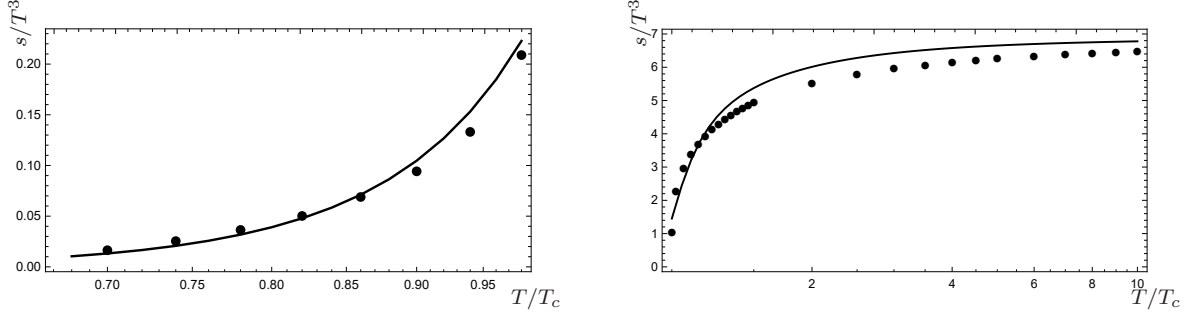


Figure 10: The same as in Fig. 9 but for the entropy density.

analytically, and this work is planned for the future.

For $T > T_c$ we are using two main dynamical effects, the Polyakov loops $L_{\text{adj}}(T)$, which are shown to enter linearly in $P(T)$, and CM confinement yielding CM screening mass, and reducing the pressure from the upper limit of the Stefan-Boltzmann law. In doing so we are using the slightly higher Debye mass, $M_0 \simeq 2m_D \simeq 4\sqrt{\sigma_s}$, however the results for the proper value of m_D do not differ much. For Polyakov lines $L_{\text{adj}}(T)$ we are using equations (56), (57), which are close both to the analytic forms obtained earlier in Eqs. (53), (54), and to the lattice data from [44].

With these modest input data we have obtained results for $P(T)$, $I(T)$ and $s(T)$, which are shown in Figs. 4-10, demonstrating a good agreement with the lattice data [25].

The same is true for the value of $T_c \simeq 260$ MeV, found from Fig. 6. Summarizing, one can say, that the confining and nonconfining dynamics considered here, is supported by independent numerical data, and can be used to develop further our approach in application to the real QCD ($n_f = 2 + 1$), as well as to the interesting cases of $n_f = 2$ and arbitrary N_c . The work of M.S.L. and Yu.A.S. was done in the framework of the scientific program of the Russian Science Foundation, RSF, project 16-12-10414.

Appendix

The V_1 cancellation in the confinement region

As it was shown in (5), the instantaneous $q\bar{q}$ interaction can be written as

$$V_{q\bar{q}}(r) = V_{\text{lin}}(r) + \bar{V}_{\text{sat}}(r), \quad (\text{A.1})$$

where

$$V_{\text{lin}}(r) = 2r \int_0^r d\lambda \int_0^\infty d\nu D^E(\lambda, \nu), \quad (\text{A.2})$$

and the saturated at large r potential $\bar{V}_{\text{sat}}(r)$ is

$$\bar{V}_{\text{sat}}(r) = \int_0^r \lambda d\lambda \int_0^\infty d\nu [D_1^E(\lambda, \nu) - 2D^E(\lambda, \nu)]. \quad (\text{A.3})$$

In what follows we show, that $\bar{V}_{\text{sat}}(r)$ is strongly suppressed in the confining region due to cancellation of D_1^E and D^E , while it is equal to $V_1(r) \equiv \int_0^r \lambda d\lambda \int_0^\infty d\nu D_1^E(\lambda, \nu)$ in the deconfined region, and $V_1(r) = V_1^{(np)} + V_1^{\text{pert}}$.

To this end one can use the gluelump representation of the correlators D^E and D_1^E , given in [35, 37]

$$D_1^E(x) = \frac{6\alpha_s M_1 \sigma_f}{x} e^{-M_1 x} \equiv \frac{A_1 e^{-M_1 x}}{x}; \quad x = \sqrt{\lambda^2 + \nu^2}, \quad (\text{A.4})$$

with

$$\sigma_f = 0.18 \text{ GeV}^2, \quad M_1 = 1.4 \text{ GeV},$$

$$D^E(x) = \frac{g^4(N_c^2 - 1)}{2} 0.108 \sigma_f^2 e^{-M_2 x}, \quad (\text{A.5})$$

with $M_2 = 1.5 \text{ GeV}$ is the mass of the two-gluon gluelump with the account of perturbative interaction. As a result of integration in (A.3) of the forms (A.4) and (A.5) one obtains $\bar{V}_{\text{sat}}(\infty)$ in the confinement phase

$$\bar{V}_{\text{sat}}(\infty) = \frac{A_1}{M_1^2} - \frac{4A_2}{M_2^3} = (0.432 - 0.415) \text{ GeV} \cong 17 \text{ MeV}, \quad (\text{A.6})$$

for $\alpha_s = 0.4$. One can find $\bar{V}_{\text{sat}}(r)$ for finite r in the range $O(10 \text{ MeV})$.

References

- [1] H.G. Dosch, Phys. Lett. **B 190**, 177 (1987); H.G. Dosch, Yu.A. Simonov, Phys. Lett. **B 205**, 339 (1988); Yu.A. Simonov, Nucl. Phys. **B 307**, 512 (1988).
- [2] A.Di Giacomo, H.G. Dosch, V.I. Shevchenko and Yu.A. Simonov, Phys. Rept. **372**, 319 (2002);
Yu.A. Simonov, Phys. Usp. **39**, 313 (1996) [arXiv:hep-ph/9709344];
D.S. Kuzmenko, V.I. Shevchenko, Yu.A. Simonov, Phys. Usp. **174**, 3 (2004) [arXiv:hep-ph/0310190].
- [3] N. Cabibbo and G. Parisi, Phys. Lett. **B 59**, 67 (1975).
- [4] J.C. Collins and M. Perry, Phys. Rev. Lett. **34**, 1353 (1975).
- [5] Yu.A. Simonov, JETP Lett. **54**, 249 (1991), *ibid.* **55**, 627 (1992); Yu.A. Simonov, Phys. Atom. Nucl. **58**, 309 (1995) [hep-ph/9311216]; N.O. Agasian, JETP Lett. **57**, 208 (1993); N.O. Agasian, JETP Lett. **71**, 43 (2000); H.G. Dosch, H.J. Pirner, Yu.A. Simonov, Phys. Lett. **B349**, 335 (1995).
- [6] Yu.A. Simonov, in “Varennia 1995, Selected Topics in Nonperturbative QCD”, p.319, 1995 [arXiv:hep-ph/9509404].
- [7] Yu.A. Simonov, Ann. Phys. **323**, 783 (2008) [arXiv: hep-ph/0702266]; E.V. Komarov, Yu.A. Simonov, Ann. Phys. **323**, 1230 (2008) [arXiv: 0707.0781].
- [8] Yu.A. Simonov, M.A. Trusov, JETP Lett. **85**, 730 (2007); Phys. Lett. **B 650**, 36 (2007); arXiv:hep-ph/0703277.
- [9] A.V. Nefediev, Yu.A. Simonov and M.A. Trusov, Int. J. Mod. Phys. **E 18**, 549 (2009) [arXiv:0902.0125].

- [10] V.D. Orlovsky and Yu.A. Simonov, Phys. Rev. **D 89**, 054012 (2014) [arXiv:1311.1087]; ibid. **D 89**, 074034 (2014) [arXiv: 1312.4178].
- [11] V.D. Orlovsky and Yu.A. Simonov, Int. J. mod. Phys. **A 30**, 1550060 (2015).
- [12] Yu.A. Simonov, arXiv: 1605.07060 (v.3).
- [13] A.D. Linde, Phys. Lett. **B 96**, 289 (1980).
- [14] D.J. Gross, R.D. Pisarski and L.G. Yaffe, Rev. Mod Phys. **53**, 43 (1981).
- [15] E.L. Gubankova and Yu.A. Simonov, Phys. Lett. **B 360**, 93 (1995).
- [16] B. Lucini, M. Teper and V. Wenger, JHEP, **0502**, 033 (2005) [hep-lat/0502003].
- [17] A. Mykkanen, M. Panero and K. Rummukainen, JHEP, 1205, 069 (2012) [arXiv:1202.2762].
- [18] J. Fingberg, U.M. Heller, and F. Karsch, Nucl. Phys. **B 392**, 493 (1993) [arXiv:hep-lat/9208012].
- [19] G. Boyd, J. Engels, F. Karsch, E. Laermann, C. Legeland, M. Lütgemeier and B. Peterson, Phys. Rev. Lett. **75**, 4169 (1995), [arXiv:hep-lat/9506025]; Nucl. Phys. **B 469**, 419 (1996) [arXiv:hep-lat/9602007].
- [20] B. Beinlich, F. Karsch, E. Laermann, and A. Peikert, Eur. Phys. J. **C 6**, 133 (1999) [arXiv:hep-lat/9707023].
- [21] E. Braaten and R. D. Pisarski, Phys. Rev. Lett. **64** (1990) 1338.
- [22] J. O. Andersen, E. Braaten, and M. Strickland, Phys. Rev. Lett. **83** (1999) 2139 [hep-ph/9902327].
- [23] J. O. Andersen, M. Strickland, and N. Su, Phys. Rev. Lett. **104** (2010) 122003 [arXiv:0911.0676].
- [24] J. O. Andersen, M. Strickland, and N. Su, JHEP **08** (2010) 113 [arXiv:1005.1603].
- [25] Sz. Borsanyi, G. Endrödi, Z. Fodor, A.D. Katz and K.K. Szabo, JHEP, **1207**, 056 (2012) [arXiv:1204.6184 [hep-lat]].
- [26] L. Giusti and M. Pepe, arXiv:1612.00265; 1612.02337.
- [27] L. G. Yaffe and B. Svetitsky, Phys. Rev. D **26**, 963 (1982).
- [28] A. Vuorinen and L. G. Yaffe, Phys. Rev. D **74**, 025011 (2006) [hep-ph/0604100].
- [29] M. C. Ogilvie, J. Phys. A **45**, 483001 (2012) [arXiv:1211.2843 [hep-th]].
- [30] P. N. Meisinger, T. R. Miller and M. C. Ogilvie, hep-lat/0110174.
- [31] O. Andreev, Phys. Rev. D **76**, 087702 (2007) [arXiv:0706.3120 [hep-ph]].
- [32] C. Ratti, S. Roessner, M. A. Thaler and W. Weise, Eur. Phys. J. C **49**, 213 (2007) [hep-ph/0609218].

- [33] C. Ratti, M. A. Thaler and W. Weise, Phys. Rev. D **73**, 014019 (2006) [hep-ph/0506234].
- [34] S. Roessner, T. Hell, C. Ratti and W. Weise, Nucl. Phys. A **814**, 118 (2008) [arXiv:0712.3152 [hep-ph]].
- [35] Yu.A. Simonov, Phys. At. Nucl. **69**, 528 (2006) [arXiv:hep-ph/0501182];
Yu.A. Simonov, V.I. Shevchenko, Adv. High Energy Phys. **2009**, 873051 (2009) [arXiv:0902.1405];
Yu.A. Simonov, Proc. of the Steklov Inst. of Math. **272**, 234 (2011) [arXiv:1003.3608].
- [36] I. Jorysz, C. Michael, Nucl. Phys. **B 302**, 448 (1988);
N. Campbell, I. Jorysz and C. Michael, Phys. Lett. **B 167**, 91 (1986).
- [37] Yu.A. Simonov, Nucl. Phys. **B 592**, 350 (2001) [arXiv:hep-ph/0003114].
- [38] Yu.A. Simonov, Phys. Atom. Nucl. **60**, 2069 (1997); arXiv:hep-ph/9704301; Phys. Rev. D **65**, 094018 (2002); arXiv:hep-ph/0201170; Int. J. Mod. Phys. **A 31**, 1650016 (2016) [arXiv:1509.06930].
- [39] Yu.A. Simonov, Nucl. Phys. B **324**, 67 (1989); A.M. Badalian, Yu.A. Simonov, Phys. Atom. Nucl. **59**, 2247 (1996);
Yu.A. Simonov, Phys. Rev. D **65**, 116004 (2002) [arXiv:hep-ph/0203059];
A.M. Badalian, A.V. Nefediev, and Yu.A. Simonov, Phys. Rev. D **78**, 114020 (2008) [arXiv:0811.2599].
- [40] O. Kaczmarek, et. al., arXiv:hep-lat/9908010.
- [41] P. Bicudo and N. Cardoso, Phys. Rev. D **85**, 077501 (2012); arXiv:111.1317; arXiv:1608.07742.
- [42] P. Cea, L. Cosmai, F. Cuteri and A. Papa, JHEP 016, 033 (2016) [arXiv:1511.01783].
- [43] Yu.A. Simonov, Phys. Lett. **B 619**, 283 (2005) [arXiv:hep-ph/0502078].
- [44] S. Gupta, K. Hübner and O. Kaczmarek, Nucl. Phys. **A 785**, 278 (2007) [arXiv:hep-lat/0608014].
- [45] A.Di Giacomo, E. Meggiolaro and H. Panagopoulos, Nucl. Phys. **B 483**, 371 (1997);
M. D'Elia, A.Di Giacomo and E. Meggiolaro, Phys. Rev. D **67**, 114504 (2003).
- [46] A.V. Nefediev, Yu.A. Simonov, Phys. Atom. Nucl. **71**, 171 (2008) [arXiv:hep-ph/0703306].
- [47] N.O. Agasian, Yu.A. Simonov, Phys. Lett. **B 639**, 82 (2006).
- [48] N.O. Agasian, Phys. Lett. **B 562**, 257 (2003).
- [49] G. Boyd, O. Kaczmarek and F. Zantow, Nucl. Phys. **B 469**, 419 (1996) [arXiv:hep-lat/0512031].
- [50] O. Kaczmarek, F. Karsch, P. Petreczky and F. Zantow, Phys. Lett. **B 543**, 41 (2002); Phys. Rev. D **70**, 074505 (2004).

- [51] A.B. Kaidalov and Yu.A. Simonov, Phys. Lett. **B 477**, 163 (2000); Phys. Atom. Nucl. **63**, 1428 (2000) [arXiv:hep-ph/9911291].
- [52] L.D. Landau and E.M. Lifshitz, Statistical Mechanics, Part I, Vol. 5 (Pergamon, New York, 1980).
- [53] Y. Chen, A. Alexandru, S.J. Dong et al., Phys. Rev. **D 73**, 014516 (2006) [arXiv:hep-lat/0510074].
- [54] C. Morningstar and M. Peardon, Phys. Rev. **D 60**, 034509 (1999) [arXiv:hep-lat/9901004].
- [55] M. Teper, hep-th/9812187.
- [56] R. Hagedorn, Nuovo Cim. Suppl. **3**, 147 (1965).
- [57] H.B. Meyer, Phys. Rev. **D 80**, 051502 (2009) [arXiv:0905.4229 [hep-lat]].
- [58] M. Shirogane, S. Ejiri, R. Iwami, K. Kanaya and M. Kitazawa [arXiv:1605.02997 [hep-lat]].
- [59] B. Beinlich, F. Karsch and A. Peikert, Phys. Lett. **B390**, 268 (1997) [arXiv:hep-lat/9608141].
- [60] N.O. Agasian, M.S. Lukashov and Yu.A. Simonov, Mod. Phys. Lett. **A 31**, 1650222 (2016) [arXiv:1610.01472 [hep-lat]].